# RFID aided SINS integrated navigation system for lane applications

Qi Wang*

School of Computer and Software,
and
Jiangsu Engineering Center of Network Monitoring,
Nanjing University of Information Science and Technology,
Nanjing 210044, China
Email: wangqiseu@163.com
*Corresponding author

Chang-song Yang

School of Automation,
and
Jiangsu Engineering Center of Network Monitoring,
Nanjing University of Information Science and Technology,
Nanjing 210044, China
Email: c.s.yang@163.com

Shaoen Wu

Department of Computer Science,
Ball State University,
Muncie, USA
Email: swu@bsu.edu

**Abstract:** To improve the lane vehicle position accuracy, RFID technology is applied to correct the position of the SINS irregularly with label positioning. The acceleration data of the vehicle in three directions is measured by the accelerometers of the inertial measurement unit; the attitude matrix is updated in real time using the angular velocity of the gyroscope output space, and the acceleration component is transformed into the geographic coordinate system, and the acceleration of the inertial measurement unit. The data is subjected to an integral operation process to obtain a spatial displacement value of the vehicle. The real-time updating algorithm of the attitude matrix and the processing of the inertial measurement unit signal are presented. The quaternion-based algorithm is used to solve the attitude matrix as well as updating the coordinate system of the inertial navigation attitude matrix in real time. The Hilbert-Huang transform is used to filter the acceleration signal to solve the integrator saturation problem caused by the low-frequency component of the acceleration signal. The EMD algorithm based on the continuous root mean square error is applied in rejecting the low-frequency components in the signal. The simulation experiments show that the system can be reliable and high precision.

**Keywords:** radio frequency identification; RFID; strapdown inertial navigation system; SINS; attitude matrix; simulation experiments.

**Reference** to this paper should be made as follows: Wang, Q., Yang, C-s. and Wu, S. (2020) 'RFID aided SINS integrated navigation system for lane applications', *Int. J. Embedded Systems*, Vol. 13, No. 1, pp.113–120.

**Biographical notes:** Qi Wang received his PhD in Instrumental Science and Engineering from Southeast University in 2009. He has worked on inertial navigation, integrated navigation, underwater navigation and underwater terrain matching.

Chang-song Yang received his PhD in Instrumental Science and Engineering from Southeast University in 2007. He has worked on inertial navigation, integrated navigation, underwater navigation and underwater terrain matching.

Shaoen Wu is an Associate Professor of Computer Science at Ball State University, and the Director of the Intelligent Computing and Communication Systems (ICCS) research group. He is an IEEE senior member. He received a PhD in Computer Science in 2008 from Auburn University. His main research is intelligent internet of things, cyber-physical systems, and wireless and mobile networking.

## 1 Introduction

With the rapid development of precision positioning technology, the demand is becoming more and more obvious, the market is also growing, and the application occasions are also increasing (Wang et al., 2019). The most common navigation service can help people quickly make travel routes, greatly facilitating people's travel (Xu et al., 2019). To achieve these aims, the first step is to achieve real time precision positioning (RTPP). In fact, the application of RTPP is very extensive (Liu et al., 2018a). Recently, more and more demands of RTPP have been made with the development of society. There are four more practical applications:

1 Medical system, which uses RFID positioning technology to quickly locate and monitor medical equipment and assets, can greatly save the cost of hospital management and create value. At the same time, it can also be used to manage patients, facilitate hospitals to better provide services for patients, and even greatly improve doctors and nurses' quick response and response to sudden conditions of certain patients, saving lives (Liu et al., 2018b).

2 Logistics industry: the existing logistics information is barcode, and the amount of information is low. When reading, the reader must aim at the selection code, which is very close and inconvenient, and it is difficult to achieve real-time positioning.

3 Chemical products and hazardous industries: chemicals and dangerous goods need to be properly handled. If RTP technology is available in the transportation and use of these goods, they can be well monitored to prevent these goods from being misused and causing safety accidents.

4 Playgrounds, supermarkets and other places where large-scale personnel are highly concentrated, people and families will walk away every day; most of them are old people and children. Once lost, it is hard for these people to find their own family. Obviously, this situation will cause great concern to family members, especially the loss of young children, which brings unthinkable concern to parents. RTP technology can easily locate family members, and this problem will be solved (Zheng et al., 2018).

At present, global positioning system is the most widely used positioning system. Satellite positioning system can provide position information with a maximum accuracy of less than 5 m. Satellite positioning system is widely used in aviation, shipping, daily production and life, and has made great contributions to the development of the whole human society (Biswas et al., 2018). However, in indoor applications, its positioning accuracy is unsatisfactory. At the same time, when locating outdoors, if we want to build a complete and independent dedicated positioning system, its construction cost is still very high, mainly because of the construction cost of the locating end. Moreover, satellite resources are very valuable. For real-time positioning of a large number of targets, satellite resources need to be occupied uninterruptedly, which is a waste of valuable satellite resources. In recent years, many positioning methods have been proposed, such as ultra-wideband positioning, ultrasonic positioning, infrared positioning, laser positioning and so on. Of course, there is also the RFID positioning technology studied in this paper. Ultra-wideband positioning transmission speed, low power, and high security, but the communication distance is short, the performance requirements of hardware are too high. The structure of ultrasonic positioning is complex and easy to implement, but it also has obvious disadvantages:

1 it is greatly affected by multipath effect and non-line-of-sight propagation, while the general location of multipath effect and non-line-of-sight propagation will encounter, which is difficult to avoid

2 the cost of building the system is very high and the economic benefit is relatively low.

Infrared positioning can be used in harsh conditions, and the accuracy is not too high. Laser positioning accuracy is very high, but the target to be positioned must be visible from the horizon, and the hardware cost is very high. Compared with the above-mentioned positioning technologies, radio frequency identification (RFID) positioning technology has the characteristics of non-contact, high stability, fast positioning, long recognition distance, non-line-of-sight positioning, low cost, and no manual intervention in recognition work. Because of the above advantages, the branch of RFID positioning has attracted more and more attention, and it is gradually considered to be one of the main positioning technologies in the future.

At present, some specific RFID positioning systems have been proposed at home and abroad, but all of them are indoor positioning systems, and they are positioning systems in a smaller range. The main indoor real-time positioning systems are 3D-ID, SpotON and LANDMARC. Pinpoint put forward the 3D system in 1999. It uses the positioning method of GPS system for reference. Specifically, it uses wireless local area network technology to locate and uses radio frequency ring time to locate. If the mobile tag receives the recognition signal from the reader, the mobile tag will modulate immediately and send the RFID signal. Then the reader will return according to the received mobile tag. The return RFID signal is computed by a certain algorithm and the azimuth is obtained. The error of the system is about 1–3 m, and the application place is indoor. However, according to the above description, it can be seen that the cost of building the system is very high, and the benefits brought by the system are not invested much, without economic benefits, there will be no market naturally (Hui et al., 2018).

According to the RSSI value of the tag to be located received by the reader, the system uses aggregation algorithm to get the orientation of the tag to be located. One of the most important advances of SPotON positioning system is the realisation of object positioning in

three-dimensional space. However, so far, a complete SPotON positioning system has not been built.

In 2003, the LANDMARC positioning system was proposed jointly by the University of Science and Technology of Hong Kong and the University of Michigan.

This system is a milestone in the development of the branch of RFID positioning system. For the first time, the system proposed the concept of active reference tags (ART), and successfully applied it to the city positioning system of RFIDs. It has achieved better positioning accuracy, which makes the real practicability and feasibility of the RFID positioning system obvious. The idea of core is to compare the RSSI values of the tags to be located and the reference tags read by multiple readers, get the neighbour reference tags needed for the location tags, and then calculate the orientation based on the known position information of the reference tags (neighbour reference tags) determined by residual weighting algorithm.

During the normal operation of the track, it is necessary for the work maintenance personnel to use professional testing equipment to conduct regular inspection of the track line to ensure the safety of the vehicle running on track. At present, dynamic detection (Qu et al., 2018) is the research and development direction of the technology in various countries in the world.

The high precision accelerometer, gyroscope, inclinometer and displacement meter are used to measure the movement of the vehicle body, the roll inclination angle, etc., and the computer is used to calculate a large amount of test data to obtain more accurate track irregularity data. The track inspection vehicle has high comprehensive performance, high detection precision, fast detection speed, high intelligence and high detection reliability. The detection method adopted by the track inspection vehicle is mainly the inertial method (Wang et al., 2015) and the chord surveying method, where the inertia can obtain the real orbit state information, but it is greatly affected by the detection speed, and is not suitable for low-speed detection, however, the chord surveying (Xia et al., 2011; Zhu et al., 2012) is independent of the inspection speed of the track inspection vehicle, but the frequency transfer function is not constant 1 which cannot reflect the irregularity of the track tread.

The strapdown inertial technology of autonomous navigation is applied to the track irregularity detection, and a strapdown inertial system is designed for track irregularity detection. The inertial navigation system combined with RFID positioning technology realises the measurement of track direction and mileage error correction. The track line is described in the direction mileage coordinate. The portable vehicle is used as the detection vehicle of the inertial measurement unit to realise the dynamic detection of the track state. The light track inspection vehicle has its own power and is electrically driven, which causes the operation is simple and convenient.

## 2 Principle of inertial navigation technology

To facilitate the establishment of the model, the geographic coordinates $O_eX_tY_tZ_t$ ($t$ system) and vehicle coordinate system $O_eX_tY_tZ_t$ ($b$ system) is defined, the origin of the system $O$, which included in the $t$ system, sets at the centre of the vehicle, the position of $OX_t$, $OY_t$, $OZ_t$ along the carries is located in the horizontal direction of the east, meridian direction north, perpendicular to the horizon. According to the geographical location of the origin of reference system, the correctness of the results of navigation calculation is independent of the definition of coordinate system orientation. In $b$ system, the centre of gravity of the inertial measurement unit is used as the origin of the vehicle coordinate system, and the direction of the axis of the $O_eX_b$ is perpendicular to the left and right sides of the track, and the longitudinal direction of the vehicle is along the $O_eX_b$, and the $O_eZ_b$ is perpendicular to the direction of the track. The vehicle coordinate system is used to determine the angular position of the track inspection vehicle relative to the local geographic coordinate system. The existence of the track irregularity is that when the vehicle is running on the track, roll, pitch and rocking occur, and the vehicle coordinate system and the vehicle body should fixed connection, using attitude angle to represent $b$ system relative to $t$ system. The state determined by the system is shown in Figure 1.

**Figure 1** Conversion between geographic coordinate and vehicle coordinate

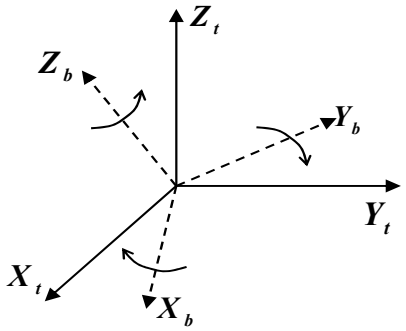


The attitude matrix (Xiang et al., 2010) is updated by using the gyroscope to measure the output angular velocity of the vehicle. The attitude matrix is the core attitude matrix of the strapdown inertial system (Qu et al., 2013; Zhou et al., 2009) to determine the accuracy of the navigation algorithm of the strapdown inertial navigation system (SINS). When solving the differential equations of attitude matrix, the quaternion method has high precision, no singularity, small arithmetic calculation, easy to program, and satisfies the attitude matrix updating algorithm of the detection system. The quaternion method is commonly used to describe the relationship of the dynamic coordinate system with respect to the orientation of the reference coordinate system. The vector portion of the quaternion can be used to represent the direction of rotation of the axis, and its scalar portion can represent half the cosine of the corner size, so it is also referred to as a rotating quaternion.

The method of rotating coordinates (Xu et al., 2017; Wu, 2010) indicates the rotation of the vehicle coordinate system relative to the geographic coordinate system:

$$Q = q_0 + q_1 i + q_2 j + q_3 k \tag{1}$$

In formula (1), $q_0$, $q_1$, $q_2$, $q_3$ are the real numbers, $i$, $j$, $k$ are the orthogonal basis. The differential expression of the quaternion is:

$$\begin{aligned} Q &= \frac{1}{2} Q \cdot \omega_{tb}^{b} \\ \omega_{tb}^{b} &= 0 + \omega_{tb}^{bk} i + \omega_{tb}^{by} j + \omega_{tb}^{bz} k \end{aligned} \tag{2}$$

In formula (2), $\omega_{tb}^{b}$ is the angular velocity vector of the $b$ system which compared to the $t$ system. The matrix form of the quaternion expression is:

$$\begin{bmatrix} \dot{q}_0 \\ \dot{q}_1 \\ \dot{q}_2 \\ \dot{q}_3 \end{bmatrix} = \frac{1}{2} \begin{bmatrix} 0 & -\omega_x^b & -\omega_y^b & -\omega_z^b \\ \omega_x^b & 0 & \omega_z^b & -\omega_y^b \\ \omega_y^b & -\omega_z^b & 0 & \omega_x^b \\ \omega_z^b & \omega_y^b & -\omega_x^b & 0 \end{bmatrix} \begin{bmatrix} q_0 \\ q_1 \\ q_2 \\ q_3 \end{bmatrix} \tag{3}$$

In formula (3), $\omega_x^b, \omega_y^b, \omega_z^b$ indicate the angular rate of the measurement of the inertial measurement unit ($x$, $y$, $z$) in the vehicle coordinate system.

The quaternion is used as the rotation of the detection. $Q_0$ is the initial time, and $Q$ is a fixed unit quaternion, which requires the following conditions:

$$q_0^2 + q_1^2 + q_2^2 + q_3^2 = 1 \tag{4}$$

There is an error in the actual mathematical operation, the above formula (4) is no way to achieve it, so $W$ must be normalised.

$$Q = \frac{q_0 + q_1 i + q_2 j + q_3 k}{\sqrt{q_0^2 + q_1^2 + q_2^2 + q_3^2}} \tag{5}$$

The relationship between the pose matrix and the quaternion is:

$$T_b^t = \begin{bmatrix} q_0^2 + q_1^2 - q_2^2 - q_3^2 & 2(q_1 q_2 - q_0 q_3) & 2(q_1 q_3 + q_0 q_2) \\ 2(q_1 q_2 + q_0 q_3) & q_0^2 - q_1^2 + q_2^2 - q_3^2 & 2(q_2 q_3 - q_0 q_1) \\ 2(q_1 q_3 - q_0 q_2) & 2(q_2 q_3 + q_0 q_1) & q_0^2 - q_1^2 - q_2^3 - q_3^2 \end{bmatrix} \tag{6}$$

The acceleration value is converted from the vehicle coordinate system to the geographic coordinate system. According to the formula $\dot{Q} = \frac{1}{2} Q \cdot \omega_{tb}^{b}$, we can calculate the value of the quaternion and obtain the attitude matrix $(T_b^t)$ for updating the attitude information in real time, which can realise the coordinate conversion of the acceleration signal.

$$\begin{bmatrix} a_x^t \\ a_y^t \\ a_z^t \end{bmatrix} = T_b^t \begin{bmatrix} a_x^b \\ a_y^b \\ a_z^b \end{bmatrix} \tag{7}$$

In this paper, the fourth Runge-Kutta (Xiong and Shi, 2018) method is used to solve the quaternion. The expression of the quaternion differential equation is:

$$Q(t+T) = Q(t) + \frac{T}{6}(k_1 + k_2 + k_3 + k_4) \tag{8}$$

In formula (8), $T$ is the time interval. In this paper, we can set $M$ for $\omega_{tb}^{b}$ inverse matrix:

$$\begin{aligned} k_1 &= \frac{1}{2} M(t) Q(t) \\ k_2 &= \frac{1}{2} M\left(t + \frac{T}{2}\right)\left[Q(t) + \frac{k_1}{2} T\right] \\ k_3 &= \frac{1}{2} M\left(t + \frac{T}{2}\right)\left[Q(t) + \frac{k_2}{2} T\right] \\ k_4 &= \frac{1}{2} M(t+T)\left[Q(t) + k_3 T\right] \end{aligned} \tag{9}$$

In this paper, the integral filter (Yao, 2005; Shu, 2016) is based on the rectangular method to estimate the transfer function of the integral filter. The vertical vibration velocity of the measured entity at the current sampling moment is $f'(n)$ and the vertical vibration acceleration is $f''(n)$, and then the vertical vibration displacement expression of the object at the current sampling time is:

$$f(n) = \frac{f''(n-2) T_n T_{n-1}}{\left(1 - z^{-1}\right)^2} \tag{10}$$

In formula (10), $T_n$ is two adjacent sampling intervals, $T_{n-1}$ is the previous value of $T_n$, $f''(n-2)$ is $f''(n)$ ahead of two sampling intervals.

**Figure 2** Integration schematic diagram (see online version for colours)

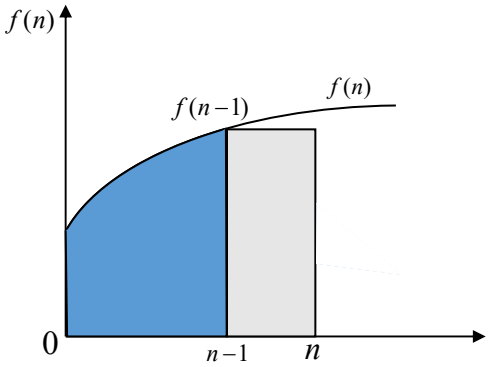


Figure 2 is the integration schematic diagram. The shaded area on the left side of the function is $f(n-1)$, and then the rest can be expressed as equation (11):

$$\Delta f(n) = f(n) - f(n-1) \approx f'(n-1) T_n \tag{11}$$

With the above formula and integral definition, you can get the following relationship:

$$f(n) = \sum_{i=0}^{n} \Delta f(i) \approx f(n-1) + f'(n-1) T_n \tag{12}$$

Organise the following relationship:

$$\begin{aligned} f(n)-f(n-1)&=f'(n-1)T_n \\ f'(n-1)-f'(n-2)&=f''(n-2)T_{n-1} \end{aligned} \tag{13}$$

Obtained by the above two formulas:

$$f(n)=\frac{f''(n-2)T_nT_{n-1}}{\left(1-z^{-1}\right)^2} \tag{14}$$

According to equation (14), the system transfer function of the second-order discrete integral filter:

$$H_z=\frac{z^{-2}\Delta T_{n-1}\Delta T}{\left(1-z^{-1}\right)^2} \tag{15}$$

## 3 Integrated navigation system based on RFID

Installed on the wheel axle, the photoelectric encoder sends a pulse signal, accumulates the mileage of the vehicle, and corrects the mileage by reading the electronic tag information at the mileage correction point to realise accurate positioning of the track geometric irregularity information on the line (Sukkarieh et al., 1999).

The specific implementation method of the integrated system is as follows: the passive electronic tags are fixedly placed in the middle position of the track sleepers at regular intervals (0.5km), and the tag reader is installed in the middle of the horizontal direction of the bottom of the car body of the detecting vehicle to make sure the reader is always above the passive electronic tag for optimal reading. During the vehicle operation, the reader moves with the vehicle and transmits the encrypted data vehicle signal to the outside through the transmitting antenna. When the reader reaches the electronic tag near the movement of the vehicle and the electronic tag enters the reading and writing range of the reader, the vehicle signal transmitted by the reader activates the electronic tag, and the electronic tag cyclically transmits the electronic tag information to the reader, and the reader receives the electronic tag. The transmitted signal is demodulated and decoded to obtain electronic tag information, and the validity of the information is determined. The valid electronic tag information is sent to the onboard computer connected to it through the RS-232 serial port (Li and Zhao, 2011).

**Figure 3** Schematic diagram of positioning system

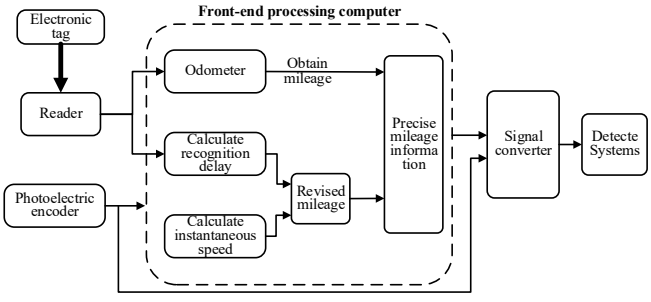


After the vehicle computer obtains the electronic tag mileage data information through the RFID reader, the tag information is compared with the pre-stored information in the mileage data table (Yan et al., 2013; Ma and Hao, 2018), the mileage information corresponding to the tag number and the line feature point information are identified, and the accumulated mileage information is corrected to get more accurate mileage information.

The empirical mode decomposition (EMD) (Zhang et al., 2015; Zhu et al., 2014) algorithm is the core algorithm of Hilbert-Huang transform (HHT), that is, through a large number of mathematical simulations, the poor performance signal is decomposed into a better performance IMF. The specific calculation steps are as follows.

First, for the original data sequence $x(t)$, Using a cubic spline interpolation function (Zhang et al., 2012; Jiang et al., 2005) to all the maxima and minima points are respectively fitted to the upper envelopes of the original data ($x_{\max}(t)$) and lower envelopes of the original data ($x_{\min}(t)$). The mean value of the upper and lower envelopes is recorded as $m_1(t)$. Sequence $x(t)$ and mean $m_1$ subtraction to get a new sequence $h_1 = x(t) - m_1$, and then correct $h_1$ repeat the above calculation process $k$ times, get the first intrinsic mode function component $c_1$, which means the highest frequency component of the signal data sequence (Meng et al., 2018; Wei et al., 2017).

Second, the original data sequence $x(t)$ and the first intrinsic mode function component $c_1$ subtraction to get a new data sequence $r_1$, and then remove the sequence of high frequency components; continue to perform the above calculation to obtain the second intrinsic mode function component $c_2$; and repeat the above decomposition process to finally obtain an indecomposable data sequence $m$, which is the trend or mean of the original data sequence $x(t)$.

The algorithm flow chart is shown in Figure 4.

**Figure 4** EMD algorithm flow chart

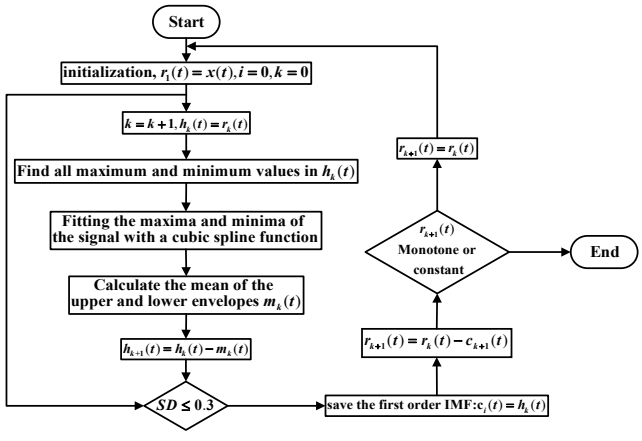


The calculation formula of SD is equation (16) which can judge whether its value exceeds the given limit; the value of this paper is set to 0.3.

$$SD=\frac{\sum\left[h_k(t)-h_{k-1}(t)\right]^2}{\sum\left[h_{k-1}(t)\right]^2} \tag{16}$$

According to the above principle, we can decompose the signal $x(t)$ and get several *IMF*. The component has a frequency from high to low and the sequential high frequency component of the signal is small, and the low frequency component is large.

The decomposed *IMF* exists the $IMF_k$ component. The noise is the dominant mode in $IMF_1$~$IMF_k$ component, however, the signal is the dominant mode in $IMF_{k+1}$~$IMF_n$ component. The ultimate goal of the decomposition method is to find the demarcation point $k$ as the demarcation point of the dominant mode of the signal and the dominant mode of the noise. The method is the *EMD* based on continuous mean square error (Zhao et al., 2018; Li et al., 2017), $k$ defined in formula (17).

$$k = \arg\min_{1\le k\le N}\left[CMES\left(\tilde{x}, \tilde{x}_{k+1}\right)\right]+1 \tag{17}$$

where

$$\begin{aligned} CMES\left(\tilde{x}, \tilde{x}_{k+1}\right) &= \frac{1}{N}\sum_{i=1}^{N}\left[\tilde{x}_k\left(t_i\right)-\tilde{x}_{k+1}\left(t_i\right)\right]^2 \\ &= \frac{1}{N}\sum_{i=1}^{N}\left[IMF_k\left(t_i\right)\right]^2, \quad k=1,\ldots,n-1 \end{aligned} \tag{18}$$

The *IMF* component in some signal dominate mode may have energy that lower than the noise mode which becomes the global minimum. When the above occurs,

$$k = \arg\, firstlocal\min\left[CMES\left(\tilde{x}, \tilde{x}_{k+1}\right)\right]+1 \tag{19}$$

The formula (19) is the method of *EMD* based on the continuous mean square error which can remove noise. The method is mainly to filter out low frequency components in the signal $IMF_{k+1}$~$IMF_n$ component, and reconstruct the components of $IMF_1$~$IMF_k$, which is the formula (20), As a result, the reconstructed signal completes the noise reduction process.

$$\tilde{x}_k = \sum_{i=1}^{k} IMF_i(t) \tag{20}$$

According to the design of the system, the working distance between the directional antenna and the passive tag of the reader is 20 cm; the low frequency (LF30~300 KHz) RF product is suitable for close-range identification (distance less than 1 m), and can penetrate most other materials except metal. The article does not reduce the reading distance, and the read/write area of the reader is more evenly distributed. Under normal circumstances, the low frequency operating frequency of RFID is 125 KHz and 134.2 KHz. (Zhou et al., 2012).

In this paper, the working frequency of RFID positioning system is 125 kHz. The working module of RFID reader includes communication module, RF module, control module, power module and interface module. The system function block diagram is shown in Figure 5.

**Figure 5** RFID reader schematic

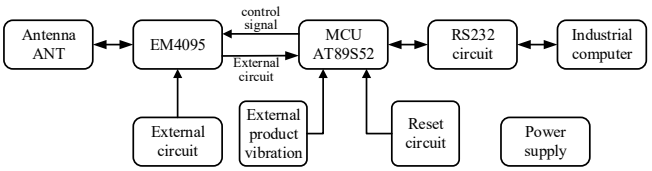


The reader chip of RFID adopts EM4095, which is a special chip of low frequency reader designed by EM Company. Its working frequency is 100~150 kHz, the working voltage is 5 V, and the EM4095 chip does not need external crystal oscillator. The interface between the EM4095 and the microcontroller is simple. The SHD should be high after the chip is powered on, initialise the chip, and then connect to the low level, that is, transmit the RF signal. The AM signal on the antenna carries a digital signal, and the demodulation module acquires the digital signal on it and outputs it through the DEMOD_OUT terminal. The reference clock signal RDY/CLK output by the EM4095 is connected to T0 and used as the decoded synchronous clock. The AT89S52 receives information from the tag, uses the MAX232 to achieve level changes, and finally communicates with the industrial computer.

## 4 Simulation experiments and results

When a lane vehicle is running, it will be shocked and oscillated by the rail. Therefore, the horizontal angle and heading angle of the vehicle will oscillate with a certain amplitude and period, and will sail at a constant speed according to a certain heading. This kind of motion condition can reflect the motion state of the ship more truthfully.

Let the ideal attitude angle be

$$\begin{cases} S\theta = A_\theta \sin\left(\omega_\theta t+\beta_\theta\right) \\ S\gamma = A_\gamma \sin\left(\omega_\gamma t+\beta_\gamma\right) \\ S\varphi = \phi_{\varphi 0}+A_\varphi \sin\left(\omega_\varphi t+\beta_\varphi\right) \end{cases} \tag{21}$$

Let the velocity be

$$\begin{cases} SV_E = SV\sin\left(S\phi_u\right) \\ SV_N = SV\cos\left(S\phi_u\right) \\ SV_U = 0 \end{cases} \tag{22}$$

where $A_\gamma$, $A_{\phi_e}$, $A_\theta$ is the swing amplitude, is 2°, 1°, 1°, respectively. Swing periods $T_\varphi$, $T_\theta$, $T_\gamma$ are 0.5 s, 0.2 s, 0.3 s, respectively, the initial phase is zero, the initial heading is 45°, constant speed is 20m/s, attitude updating period is 10 ms.

The vehicle motion model is a three-axis sinusoidal wave combination swing motion. The selection of its amplitude, period and phase should be as close as possible to the actual system swing test. Here, the error of inertial instruments is increased. The initial simulation conditions are as follows:

In strapdown positioning system, the random drift of gyroscopes in three directions is all 0.05(°)/h, constant drift is 0.1(°)/h; the random bias of accelerometer is 50 ug, constant bias is 50 ug; the initial alignment angle is as follows, heading angle is 0.15°, pitching angle is 0.15°, rolling angle is 0.15°.

The strapdown inertial navigation system assisted by RFID radio frequency positioning can converge the position and velocity information of strapdown inertial navigation system. It can meet the requirements of autonomous lane navigation. From the simulation experiments, we can see that under the dynamic conditions, the navigation positioning accuracy is higher, the speed accuracy is about 0.1 m/s, and the position accuracy is less than 5 cm.

**Figure 6** Eastern velocity error (see online version for colours)

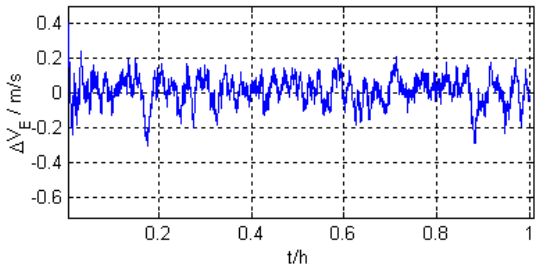


**Figure 7** Northern velocity error (see online version for colours)

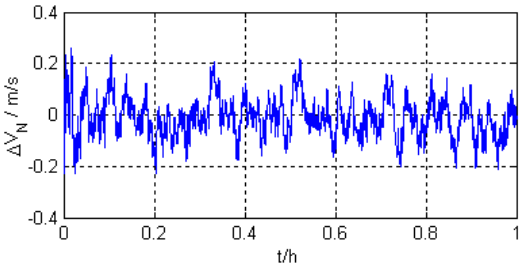


**Figure 8** Pitching angle error (see online version for colours)

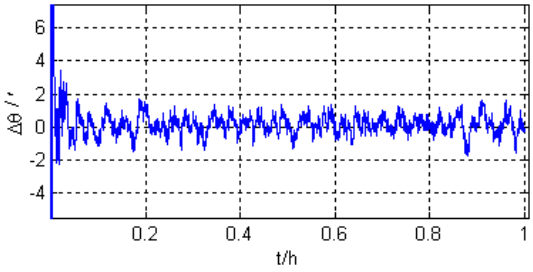


**Figure 9** Rolling angle error (see online version for colours)

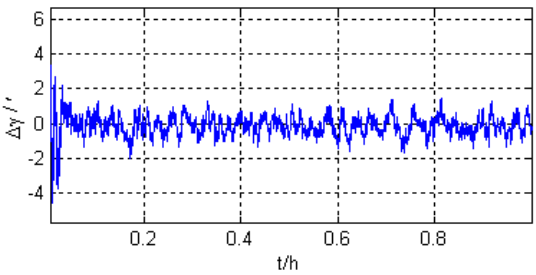


**Figure 10** Heading angle error (see online version for colours)

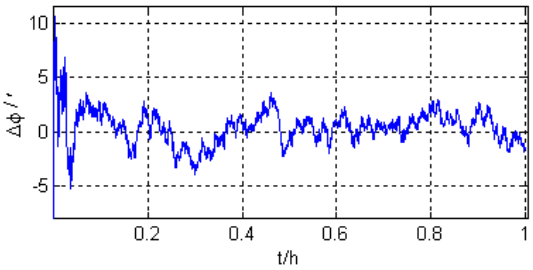


## 5 Conclusions

Due to the characteristics of high precision autonomous navigation for lane vehicles, because SINS has high short-term accuracy and accumulates errors over time, the accuracy of RFID positioning system is not affected by time and does not accumulate error with time. A strapdown integrated navigation system based on fuzzy adaptive Kalman filter is proposed, which integrates the position information provided by RFID system with strapdown navigation system. The system can make up for the shortcomings, optimise the configuration and get the optimal output, which enhances the security and improves the accuracy of long-distance navigation. SINS/RFID integrated navigation technology effectively overcomes the shortcomings of SINS navigation error accumulated over time. In practical engineering applications, SINS always maintains high positioning accuracy by relying on RFID to provide positioning correction for SINS.

## Acknowledgements

This work is funded by Natural Science Foundation of Jiangsu Province under Grant BK20160955, a project funded by the Priority Academic Program Development of Jiangsu Higher Education Institutions and Science Research Foundation of Nanjing University of Information Science and Technology under Grant20110430. Open Foundation of Jiangsu Key Laboratory of Meteorological Observation and Information Processing (KDXS1304), Open Foundation of Jiangsu Key Laboratory of Ocean Dynamic Remote Sensing and Acoustics (KHYS1405).

## References

Biswas, A., Biswas, B., Kumar, A. and Mishra, K.K. (2018) 'Particle swarm optimisation with time varying cognitive avoidance component', *Int. J. Computational Science and Engineering*, Vol. 16, No. 1, pp.27–41.

Hui, Z., Liyan, X. and Jianjun, C. (2018) 'The intensional semantic conceptual graph matching algorithm based on conceptual sub-graph weight self-adjustment', *Int. J. Computational Science and Engineering*, Vol. 16, No. 1, pp.53–62.

Jiang, Y.S., Zhang, C. and Lin, J.Y. (2005) 'Radio frequency identification technology and its application and development trends', *Application of Electronic Technique*, Vol. 31, No. 5, , pp.1–4.

Li, K., He, W., Zhang, Z. and Zhou, Q. (2017) 'Node localisation for wireless networks in smart distribution automation', *Int. J. Sensor Networks*, Vol. 23, No. 1, pp.53–60.

Li, Y. and Zhao, Z. (2011) 'Research on the method of positioning correction for field navigation vehicles based on Kalman filter', *Agricultural Equipment and Vehicle Engineering*, Vol. 49, No. 9, pp.3–9.

Liu, B., Dong, H. and Qian, S.Y. (2018a) 'Ultrasonic signal denoising method based on empirical mode decomposition and wavelet analysis', *Journal of Test and Measurement Technology*, Vol. 32, No. 5, pp.422–428.

Liu, Q., Li, S., Liu, X. and Linge, N. (2018b) 'A method for electric load data verification and repair in home environment', *International Journal of Embedded Systems*, Vol. 10, No. 3, pp.248–256.

Liu, Z., Jia, W. and Wang, G. (2018c) 'Area coverage estimation model for directional sensor networks', *International Journal of Embedded Systems*, Vol. 10, No. 1, pp.13–21.

Ma, X. and Hao, Y.N. (2018) 'Research on decompassing method of empirical mode decomposition', *Science and Technology Vision*, Vol. 23, pp.72–73.

Meng, R., Rice, S., Wang, J. and Sun, X. (2018) 'A fusion stenographic algorithm based on faster R-CNN', *CMC: Computers, Materials & Continua*, Vol. 55, No. 1, pp.1–16.

Qu, F., Li, T., Xie, A. and Kong, Q. (2013) 'Application of wireless sensor networks in military', *Electronic Design Engineering*, Vol. 21, No. 15, pp.34–36.

Qu, Z., Zhu, T., Wang, J. and Wang, X. (2018) 'A novel quantum steganography based on brown states', *CMC: Computers, Materials & Continua*, Vol. 56, No. 1, pp.47–59.

Shu, C. (2016) 'Research and verification of road condition optimization for floating vehicle based on WSN and GNSS fusion positioning', *Traffic Standardization*, Vol. 2, No. 4, pp.62–71.

Sukkarieh, S., Nebot, E.M. and Durrant-Whyte, H.F. (1999) 'A high integrity IMU/GPS Navigation loop for autonomous land vehicle applications', *IEEE Transactions on Robotics and Automation*, Vol. 15, No. 3, pp.572–578.

Wang, Q., Yang, C., Wu, S. and Wang, Y. (2019) 'Lever arm compensation of autonomous underwater vehicle for fast transfer alignment', *CMC: Computers, Materials & Continua*, Vol. 59, No. 1, pp.105–118.

Wang, Y., Xu, J.H., Chen, W., Xiao, J.L. and Wang, P. (2015) 'Study on the mathematical model of orbital irregularity accurate value based on midpoint string measurement method', *Railway Construction*, Vol. 55, No. 5, pp.139–143.

Wei, X., Wang, X., Bai, X., Bai, S. and Liu, J. (2017) 'Autonomous underwater vehicles localisation in mobile underwater networks', *Int. J. Sensor Networks*, Vol. 23, No. 1, pp.61–71.

Wu, H. (2010) 'Research on fusion localization algorithm of GNSS and wireless sensor network', *Computer Simulation*, Vol. 26, No. 11, pp.145–148.

Xia, B.G., Wang, W.D. and Wang, D.Y. (2011) 'Application of radio frequency (RFID) technology in high-speed detection of vehicle precise positioning', *Railway Construction*, Vol. 13, No. 51 ,pp.102–106.

Xiang, F.T., Wang, Z.Z., Wu, D.Z. and Yue, D. (2010) 'A precise integration method for quaternion gesture solving of strapdown system', *Journal of Sichuan Institute of Ordnance Engineering*, Vol. 31, No. 5, pp.103–106.

Xiong, L. and Shi, Y. (2018) 'On the privacy-preserving outsourcing scheme of reversible data hiding over encrypted image data in cloud computing', *CMC: Computers, Materials & Continua*, Vol. 55, No. 3, pp.523–539.

Xu, J., Ma, N., Ke, J., Yang, J. and Feng, S. (2019) 'A fast video haze removal algorithm via mixed transmissivity optimisation', *International Journal of Embedded Systems*, Vol. 11, No. 1, pp.84–93.

Xu, X., Dong, Y., Tong, J. and Dai, W. (2017) 'Improved fifth-degree spherical simplex sadial cubature Kalman filter in SINS/DVL integrated navigation', *Journal of Chinese Inertial Technology*, Vol.25, No.3, pp.343-348.

Yan, J., Xu, X., Zhang, T., Liu, Y. and Wu, L. (2013) 'Design of marine-based miniature tightly integrated SINS/GNSS navigation system', *Journal of Chinese Inertial Technology*, Vol. 21, No. 6, pp.775–780.

Yao, R. (2005) 'Simulation of strapdown inertial navigation system based on MATLAB/Simulink', *Control of Microcomputer*, Vol. 21, No. 2, pp.194–195.

Zhang, T., Chen, L., Shi, H. and Hu, H. (2015) 'Underwater positioning system based on SINS/DVL and LBL interactive auxiliary for AUV', *Journal of Chinese Inertial Technology*, Vol. 23, No. 6, pp.769–774.

Zhang, T., Xu, X., Liu, X., Tian, S. and Liu, Y. (2012) 'Time synchronization on SINS/GPS integrated navigation system under different dynamic conditions', *Journal of Chinese Inertial Technology*, Vol. 20, No. 3, pp.320–325.

Zhao, X., Wu, J., Zhang, Y., Shi, Y. and Wang L. (2018) 'Fault diagnosis of motor in frequency domain signal by stacked denoising auto-encoder', *CMC: Computers, Materials & Continua*, Vol. 57, No. 2, pp.223–242.

Zheng, Y., Ma, K., Wang, S., Sun, J. and Zhang, J. (2018) 'Line integral convolution-based non-local structure tensor', *Int. J. Computational Science and Engineering*, Vol. 16, No. 1, pp.98–105.

Zhou, J., Wang, X., Zhang, R. et al. (2012) 'Location method of GNSS and DR integrated navigation system for agricultural locomotives', *Journal of Agricultural Machinery*, Vol. 43, No. 10, pp.262–265.

Zhou, J., Zhang, Man., Wang, M. et al. (2009) 'Route tracking of agricultural vehicles based on fuzzy control', *Journal of Agricultural Machinery*, Vol. 40, No. 4, pp.151–156.

Zhu, W.F., Chai, X.D., Zheng, S.B. et al. (2014) 'Acceleration signal processing of inertial measurement unit based on empirical mode decomposition', *Urban Mass Transit Research*, Vol. 17, No. 12, pp.83–85.

Zhu, W.F., Chai, X.D., Zheng, S.B., Li, L.M. and Hu, K. (2012) 'Displacement information acquisition based on integral filter', *Instrument Technique and Sensor*, Vol. 23, No. 5, pp.62–64.